Computational Model of a Conditionally Bursting Two-Cell Half-Center Oscillator: CS4590 Final Modeling Project

Zachary Noah

College of Engineering, University of Missouri – Columbia

Biology & Function

In this project we study and analyze a simulated two-cell half-center oscillator (HCO) by constructing a conductance-based computational model using NEURON. As the name suggests, an HCO is a system of two neuronal cells connected through reciprocal inhibition such that when one neuron is active the other is silent, producing an alternating oscillatory pattern. The objectives of this work are to design non-endogenous single-cell neuron models capable of spiking, adaptation, and bursting, extend them to exhibit rebound bursting under inhibitory synaptic input, and couple two identical neurons to generate stable, alternating oscillations. This alternating activity is the core function of the HCO and closely mirrors how many biological central pattern generators produce rhythmic outputs.

The HCO that is outlined in this project utilizes reciprocal inhibition to achieve this oscillation. This means that the two cells are coupled in a way such that the firing of one inhibits the firing of the other. As seen in Figure 1, each of these cells are provided a short burst of current injection in order to kick-start the cycle.

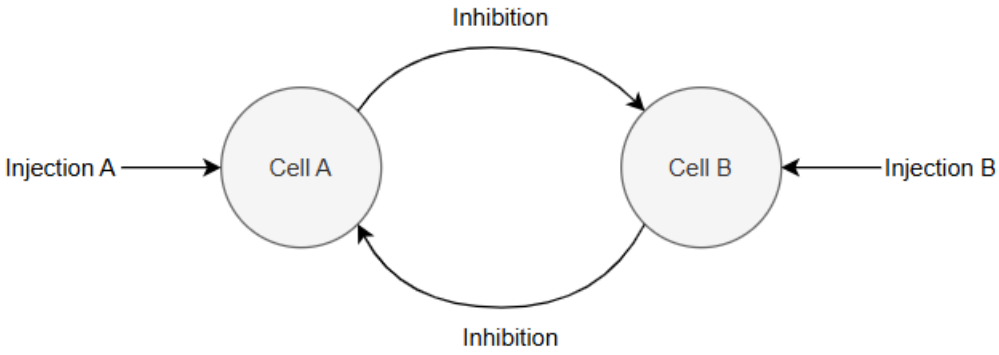

Figure 1: Abstracted diagram of system composition. Two identical neuronal cells are connected to two identical synapses of opposite directionality. A current injection is inserted into each neuronal cell.

When Cell A begins its action potential, it suppresses, or inhibits, the action potential in Cell B. When Cell A eventually ends its action potential, the newly-unsuppressed Cell B will rebound and fires in turn, consequently suppressing Cell A and completing the cycle. Because this HCO relies on mutual inhibition as the driving mechanism behind the oscillation, when these two neurons are isolated, no oscillation pattern is produced.

To create this system computationally, we begin by creating the simplest model of a neuron—one that can react to a current injection and initiate an action potential. This type of simple behavior is called ‘spiking’, and, in the case of a prolonged current injection, it will rhythmically produce action potentials. This model neuron requires integration of three ion channels, these being Na, K, and leak channels. These leak channels are always active and are crucial in maintaining the baseline membrane potential. In the case of the HCO we are building, this value is approximately -60mV. Once the current injection depolarizes the membrane to -40mV, the Na channels will open and begin to allow Na^+ ions into the cell, causing a rapid depolarization and consequently the generation of an action potential. As the membrane potential

approaches +40mV, these Na channels will begin to inactivate, and the voltage gated K channels begin to open. These K channels allow a K^+ efflux and result in a rapid repolarization of the cell, recovering the membrane potential back to a resting state.

This model can be further improved by implementing additional behaviors, one of which is the ability to "adapt". This is achieved by integrating two new ion channels Ca_S and K_{Ca}. These Ca_S channels are responsible for a slow depolarizing force and populating the cell with Ca^{2+} ions, which is crucial for the K_{Ca} channels to enable. These K_{Ca} channels activate at elevated Ca^{2+} ion concentrations and, similarly to our other K channel from before, it allows for a K^+ efflux, resulting in repolarization. The key difference with these channels is that they are not voltage-gated, but calcium-gated. This means, upon high concentrations of Ca^{2+}, these channels will open and K^+ ions can continue to leave the cell even past resting membrane potential, leading to a hyperpolarization effect. This hyperpolarization is what leads to this "adaptation" that you can see in the frequency of firing.

With the addition of this hyperpolarized state, two additional channels can be implemented, an A-type transient potassium channel and transient calcium channels. These potassium channels introduce the A-current, which, put simply, is the "brakes" on firing an action potential. These channels activate around -50mV and pump K^+ ions out of the cell and inactivate upon reaching the action potential threshold. This activation and inactivation range allows for the channels to inhibit our neuron at low depolarizations and consequently prevents small fluctuations from firing an action potential response. The transient calcium channels are responsible for the Ca_T current. They activate around -40mV and work to depolarize the neuron by encouraging Ca^{2+} ions to enter the cell. This Ca_T current forms an interesting dynamic with the previously introduced K_{Ca} current, as they drive the cell towards opposite polarization and are active in the same voltage range. In addition to having the same activation range, the Ca_T current is more active towards the negative end of the range and the K_{Ca} current is more active towards the positive end of the range. These traits end up forming a cycle in which the Ca_T elicits Ca^{2+} influx and depolarizes the cell to +40mV. At this time, the K_{Ca} responds to the Ca^{2+} presence and repolarizes to -40mV. This two-step cycle will repeat until the cell "adapts" to this pattern and hyperpolarizes. This depolarized-repolarized pattern is known as the cell "bursting".

Another essential component of the HCO is the synaptic connections. These are modeled simply as another current that activates upon the membrane potential crossing a certain threshold. When activated, it will drive the postsynaptic membrane potential toward the synaptic reverse potential, approx. -80mV in our final model. Because the synaptic reverse potential is lower than resting membrane potential of the neurons, this synapse is considered inhibitory. Additionally, the inhibited cell will be pushed to be heavily hyperpolarized. In this stated, certain currents are activated, namely the 'Hyper' current. This current acts to slowly depolarize the cell after is has been inhibited and provide a gentle inward push to help recover from inhibition. In this way, the 'Hyper' current contributes to timing of rebound bursting by determining how quickly the neurons can climb back towards threshold after being suppressed.

Math & Model

The membrane equation for a neuron will describe how the neuron's membrane potential changes over time based on its involved currents. In the neurons we designed, this simply means

that the voltage of the membrane will change corresponding to the summed currents from its ion channels, the synaptic current, and the injected current. Below is a simple mathematical description of this property.

$$C_m * \frac{dV}{dt} = I_{syn} - I_{inj} + \sum I_{ions}$$

In which I_{ions} is the set of: I_{Na}, I_{Kdr}, I_{leak}, I_{CaS}, I_{KCa}, I_{Ka}, I_{CaT}, I_{Hyper}. Because all of these ion channels have differing properties, their currents must be modeled separately. Below are the standard Hodgkin-Huxley ionic current equations with their own individual gating activation and inactivation variables.

$$I_{leak} = \bar{g}_{leak} * (V - E_{leak})$$

$$I_{Na} = \bar{g}_{Na} * m^3 * h * (V - E_{Na})$$

$$I_{Kdr} = \bar{g}_{Kdr} * n^4 * (V - E_K)$$

$$I_{KCa} = \bar{g}_{KCa} * c^4 * (V - E_K)$$

$$I_{CaS} = \bar{g}_{CaS} * ja^3 * k * (V - E_{Ca})$$

$$I_{KA} = \bar{g}_{KA} * a^3 * b * (V - E_K)$$

$$I_{CaT} = \bar{g}_{CaT} * u^3 * z * (V - E_{Ca})$$

$$I_{Hyper} = \bar{g}_{Hyper} * hm * (V - E_{Hyper})$$

One of the most dynamic parts of our model is the intracellular Ca^{2+} ion concentration. Calcium levels are crucial to monitor, as the interaction between our currents causing calcium influx and our I_{KCa} current is the key mechanism behind our 'bursting' behavior. Ca^{2+} concentration can be modeled as seen below, in which Tau_{Ca} is an arbitrary decay time constant which will be decided later.

$$\frac{d[Ca]}{dt} = -k_{Ca}\,(I_{CaS} + I_{CaT}) - \frac{[Ca]}{\tau_{Ca}}$$

The synaptic interaction between the two neurons is modeled in a systematic way similar to the ion channel currents. This means the synaptic current is treated as another conductance-based term that contributes to the membrane equation. The synaptic current is then computed as:

$$I_{Syn} = \bar{g}_{syn}(V - E_{Syn})$$

With gsyn being the synaptic conductance and Esyn being the synaptic reverse potential. Gsyn is generated by two internal variables, A and B, which each rise instantly when a spike arrives then decay exponentially with distinct time constants, tau1 and tau2 for the rapid rise and exponential decay respectively. This dual-exponential structure produces a synaptic waveform that captures a fast onset and a gradual fall often seen in inhibitory postsynaptic currents. Conductance is computed in addition to a weight w and a normalizing factor as seen below.

$$\bar{g}_{syn} = w * \bar{g}_{max} * norm * \frac{\tau_1 \tau_2}{\tau_2 - \tau_1} * (B - A)$$

Methods

Files for the computational model are composed of two main categories, the neuron model files and the python files. These neuron model files, also known as .mod files, contain what is essentially the "blueprint" behind every ionic and synaptic current that will be implemented in the model neuron. Though the exact code is a little more abstract, on a simplified level, it can be broken up into two main sections: A biological definition of the current channel and a mathematical definition of the current channel.

The biological definition of each mechanism is specified within the NEURON, PARAMETER, ASSIGNED, and UNITS sections, which together define the ions used, biophysical parameters such as conductances and time constants, the variables computed during the simulation, and the names of units associated with these quantities.

The mathematical behavior of each mechanism is specified within the STATE, DERIVATIVE, BREAKPOINT, INITIAL, and PROCEDURE sections. When combined with the definitions in the biological section, these blocks describe the differential equations, the dynamic variables they govern, the computations performed at each timestep, initial conditions, and any helper functions used for intermediate calculations.

With all of the .mod file definitions in place, the NEURON python library can be utilized to construct the functional parts of the final computational model. A class called HCOCellTemplate is created for a standalone neuronal cell blueprint using NEURON. In this class, a soma for the neuronal cell is defined with specific diameter and length. For the computational model outlined in this report, the neuron is approximately 1000 microns in length and 10 microns in diameter, resulting in an area of about 3140 microns squared. Once the soma has basic parameters defined, more advanced biophysics of the soma are implemented. This comes in the form of integrating the earlier .mod files by using NEURON's insert function alongside setting some default biophysics parameters such as conductances and reverse potentials. Additionally, some helper functions are implemented to streamline setting up the data record, plotting said record, and setting and getting biophysics.

In order to build a functional computational model, a proper testing environment with consistent parameters is necessary. Conveniently, NEURON allows for testing environment creation and running. Their standard running environment is used for this model, in which an instance of the HCOCellTemplate class is created as CellA. The running environment's general parameters, such as the time stop, initial voltage, and time step are set. CellA's attributes are then set (using the previously mentioned attribute setting helper function) according to what traits are desired for the cell to have. These neuronal traits were introduced in the order shown in Figure 2.

Figure 2: Implementation flowchart. These operations represent all steps for the "selective expression" section of the parametric study.

The only channels a spiking cell requires are Na, K, and leak channels. Because every channel is already implemented in the HCOCellTemplate class, making a spiking cell is as simple as modifying the simulation parameters as shown below.

Leak	0.0002
Na	0.55
K_{dr}	0.2
Ca_S	0
K_{Ca}	0
K_A	0
Ca_T	0
g_{Max}	0
Hyper	0

Creating an adapting cell requires implementation of Ca_S and K_{Ca} currents. Similarly, this can be done by changing simulation parameters to the following:

Leak	0.0002
Na	0.55
K_{dr}	0.2
Ca_S	0.015
K_{Ca}	0.07
K_A	0
Ca_T	0
Hyper	0

A bursting cell requires the previously mentioned A-type transient potassium channels, or K_A current, alongside a Ca_T current. Once again, this is accomplished by simply adapting simulation parameters fittingly, which is shown below.

Leak	0.0002
Na	0.55
K_{dr}	0.2
Ca_S	0.015
K_{Ca}	0.02
K_A	0.15
Ca_T	0.02
Hyper	0

Implementation of the next step, synaptic input, is more complex than just switching around some simulation parameters. Because synaptic input requires a pre-synaptic cell and a post-synaptic cell, a new neuron, CellB is created from the HCOCellTemplate class. As per Figure 1, this is the final neuron that this project will implement. Our synaptic input is achieved through two of NEURON's built-in functions, these being 'inhsyn' and 'NetCon'. 'inhsyn' simply instantiates the synaptic junction alongside the post-synaptic connection of an inhibitory

synapse. NetCon defines the pre-synaptic end of the connection alongside weights for how strong it will inhibit. One ‘inhsyn’ and ‘NetCon’ is created for each synaptic ‘Inhibition’ connection seen in Figure 1. After setting the synaptic properties and biophysics of CellB, the synaptic connections between the two cells are complete.

The final step in the development process is finalizing and fine-tuning parameters to enable a rebounding-burst pattern. A hyperpolarization current is introduced to encourage the inhibited neuron to rebound with enough force to elicit an action potential. Below is the set of parameters that were found to produce the desired results of a rebounding burst pattern.

Leak	0.0002
Na	0.55
K_{dr}	0.2
Ca_S	0.015
K_{Ca}	0.02
K_A	0.15
Ca_T	0.02
Hyper	0.001

For each cell configuration, simulations were run with both current injections and synaptic input disabled. In all cases, the membrane potential returned to resting values after an initial transient and no sustained spiking r bursting was observed, confirming the cells were not endogenous bursters.

Various supplementary codes were created to document parameters, output, etc. of the simulation to assist in visualization, debugging, and fine-tuning parameters for showcase. The creation process for such code will not be documented in this article but is available to view in the project’s Google Colab notebook accessible through the attributed GitHub.

Parametric Study Results

Parametric studies were conducted in two parts, selective expression of features and parameter sweeps. Selective expression of features provided further clarification on which ion channels play major roles in various firing patterns.

Selective Expression of Features

By limiting expressed channels to only leak, Na, and K_{Dr}, a tonically spiking cell is created. This tonic behavior will continue until the current injection is no longer affecting the neuron.

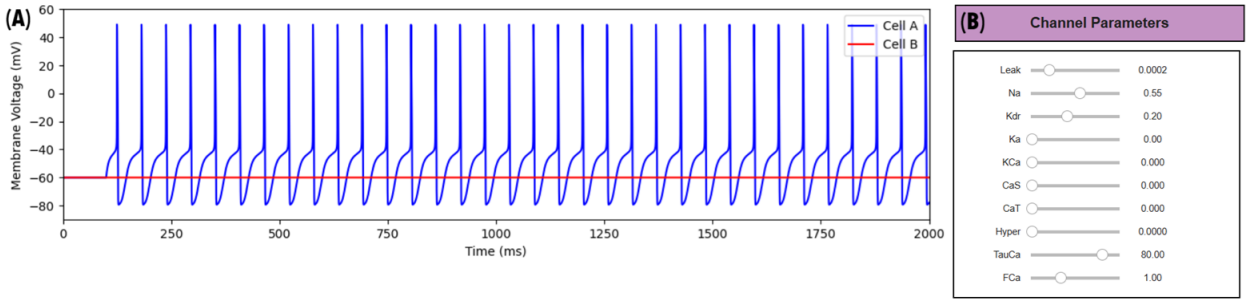

Figure 3: Output and input GUI from simulation corresponding to a tonically spiking cell. **(A)** Cell A's membrane potential is seen to tonically spike up to ~50mV then down to -80mV. **(B)** Channel conductance parameters. "Unexpressed" channels are set to 0 conductance.

Re-introducing expression of Ca_S and K_{Ca} currents modifies this behavior such that it reacts with a reduced sensitivity when subjected to a prolonged current injection. As can be observed from the Ca pool in Figure N (B), even just having these two currents is enough to create complex adapting behavior characterized by the shorter local maximums and less frequent fluctuations.

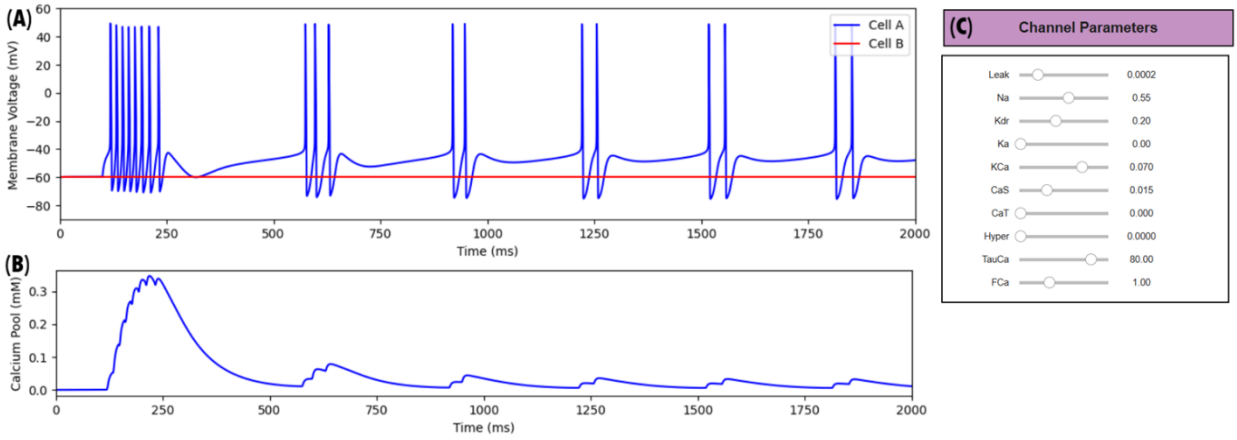

Figure 4: Output and input GUI from simulation corresponding to a cell with adapting behavior. **(A)** Cell A's membrane potential is observed spiking up to ~50mV then returning to ~-70mV with diminishing frequency. **(B)** Calcium concentration in the calcium pool is seen to closely mimic the voltage changes in directionality. **(C)** Channel conductance parameters. "Unexpressed" channels are set to 0 conductance.

Bursting behavior can be observed through implementation of Ca_T and K_A channels. This is the ability for the system to reach multiple "peaks" of the action potential without returning to baseline resting membrane potential.

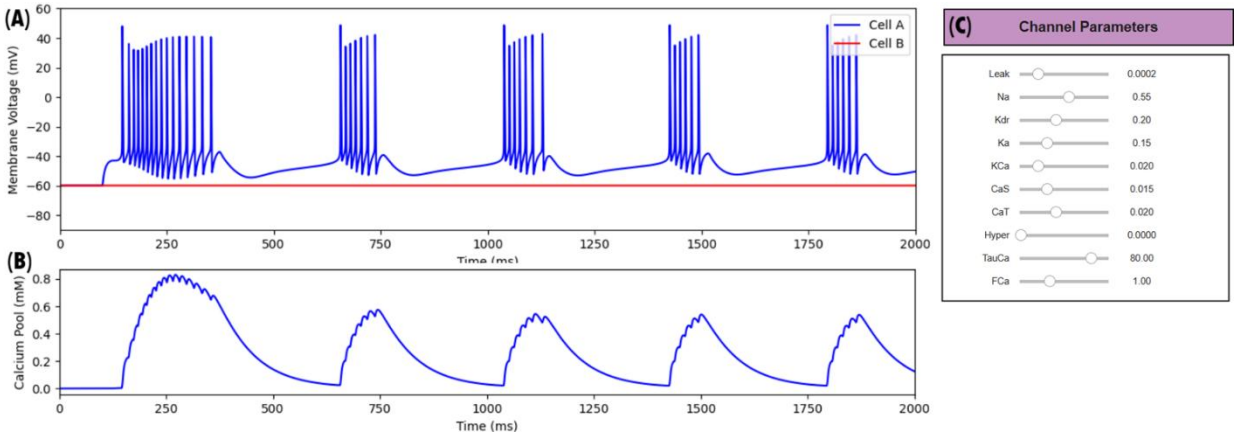

Figure 5: Output and input GUI from simulation corresponding to a cell with bursting behavior. **(A)** Cell A's membrane potential is observed bursting between ~50mV and -45mV then returning to ~-60mV with diminishing intraburst volume. **(B)** Calcium concentration in the calcium pool is seen to closely mimic the voltage changes in directionality. A more gradual change in overall directionality is seen in calcium pool dynamics at the apex of a burst compared to Figure 4 (B). **(C)** Channel conductance parameters. "Unexpressed" channels are set to 0 conductance.

Visual comparison between bursts in membrane potential and spikes in Ca pool hints at a correlation, which could, in the future, be further analyzed to potentially prove related biophysiological ideas.

By incorporating the AB synapse, the model can selectively highlight the influence of the synapse on the pre and post-synaptic cells' membrane potentials. As expected, the pre-synaptic membrane potential is not affected by incorporation of this synapse. On the other hand, the post-synaptic cell (Cell B) is observed to hyperpolarize upon the pre-synaptic cell (Cell A) firing. Current measurements for the AB synapse support this behavior.

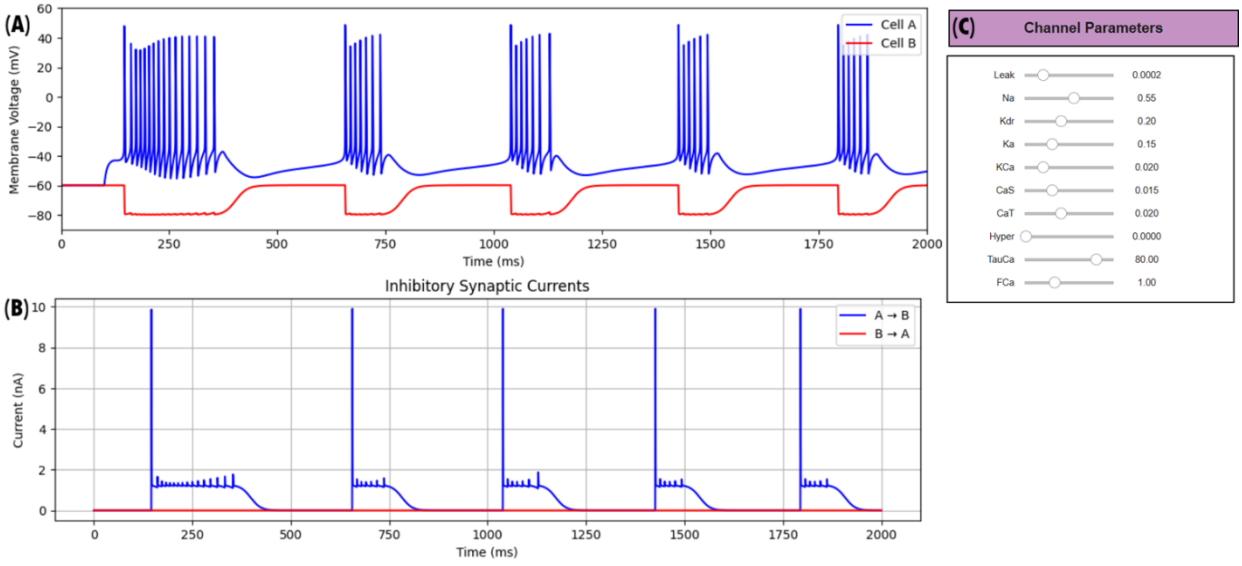

Figure 6: Output and input GUI from simulation corresponding to a cell with adapting behavior and its post-synaptic counterpart. **(A)** Cell B's membrane potential shows a stable voltage with clear recesses corresponding to heightened voltage during Cell A's bursting. **(B)** AB synaptic

currents show an increased current upon bursting of presynaptic cell. **(C)** Channel conductance parameters. “Unexpressed” channels are set to 0 conductance.

Implementation of a hyperpolarization current alongside synapse BA finalized the structure of the system and an oscillation pattern was observed. This system seems to be relying on a release-driven mechanism, as the firing of one neuron was not observed to be halted by the firing of the next but naturally exhausted.

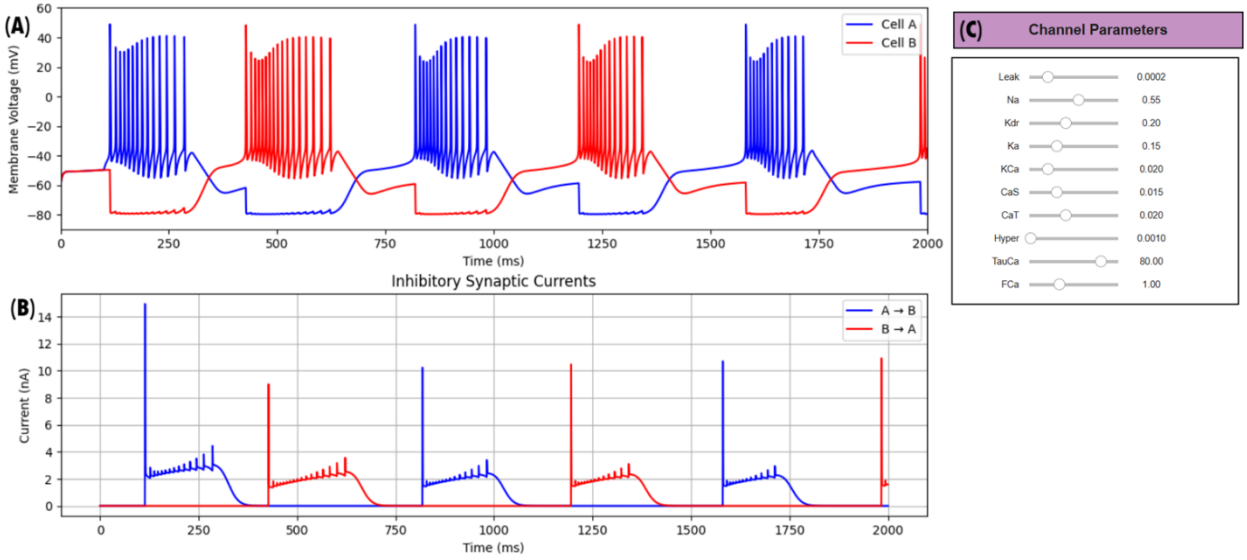

Figure 7: Output and input GUI from simulation corresponding to two cells with oscillating bursts. **(A)** Cell A is observed to begin a burst and once finished is followed by Cell B bursting. During inhibition of each cell the voltage approaches and steadily remains near synaptic reverse potential. **(B)** AB synaptic currents show an increased current upon bursting of its presynaptic cell, Cell A. BA synaptic currents mimic this same pattern for its presynaptic cell, Cell B. **(C)** Channel conductance parameters. “Unexpressed” channels are set to 0 conductance.

Parameter Sweeps

Parameter sweeps revealed critical information about the stability of the oscillating system and how each parameter functions within their respective ‘feasible’ ranges. This ‘feasible’ range is simply the minimum and maximum values for that parameter that will still generate an oscillating pattern. Large parameter sweeps were completed for every conductance, typically revealing a “plateau” shape seen in Figure 8, in which there is a steep incline in oscillation frequency upon entering this ‘feasible’ range and a steep decline upon leaving this ‘feasible’ range.

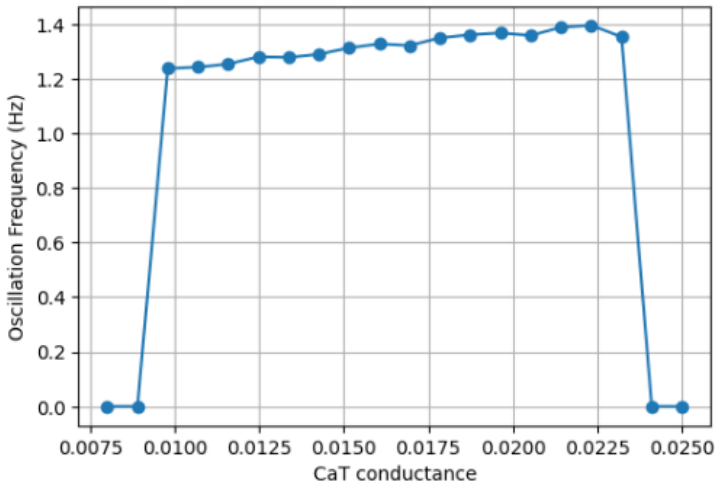

Figure 8: Graph of oscillation frequency compared to differing Ca_T conductance values. A "plateau" is formed in which there is a steep incline of oscillation frequency into this range then a steep decline in oscillation frequency out of this range.

'Feasible' ranges for each of the conductances was derived from repeating these large parameter sweeps and documenting the values of these 'drops'. Ranges for all of the channels' conductance values can be seen below.

Conductance	Feasible Minimum	Feasible Maximum
Leak	0.0001	0.0002
Na	0.49	1
K_{Dr}	0.2	0.9
K_A	0.08	0.17
K_{Ca}	0.014	0.021
Ca_S	0.0155	0.05
Ca_T	0.0009	0.023
Hyper	0.00093	0.1

Enhanced study can be performed on these ranges by clamping $\bar{g}$ values in parameter sweeps to be within these ranges of firing. This results in every channel having unique characteristics on how they effect oscillation frequency over their 'feasible' range. Tests for K_{Ca}, Ca_T, and Hyperpolarization currents resulted in an almost strictly increasing trend in conductance and oscillation frequency. A roughly negative correlation was observed between channel conductance and oscillation frequency in K_A and K_{Dr}. An inverted-U correlation was noticeable when testing leak conductance. Testing of Na channels lead to a bimodal relationship between their conductance and oscillation frequency. Complex and abnormal behavior was observed when testing Ca_S conductance, seeing frequent outliers, implying a need to refine this model before any conclusions can be made.

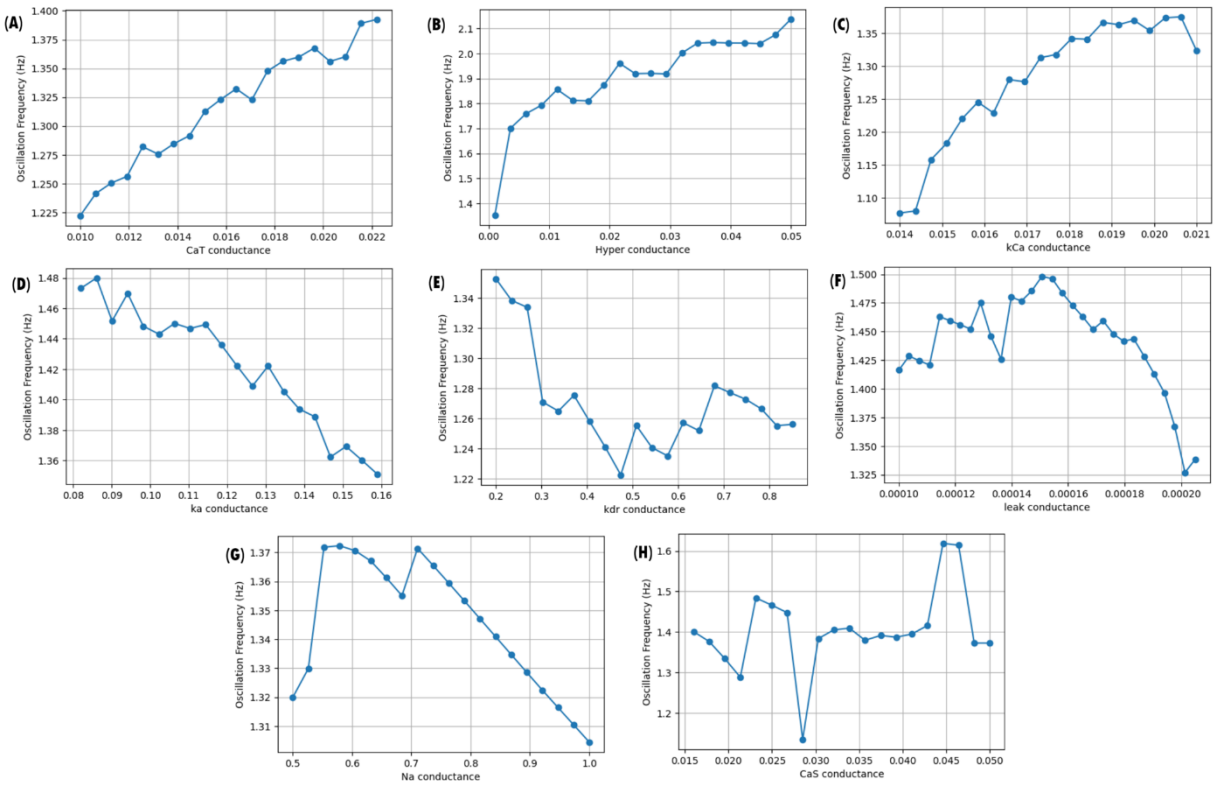

Figure 9: Graphs of oscillation frequency compared to various conductances. Conductance values of these graphs were limited to values within the "feasible" range of each conductance. **(A)** An almost linear positive correlation was noticed between Ca_T conductance and oscillation frequency. **(B)** A positive correlation was seen between Hyperpolarization conductance and oscillation frequency. **(C)** A positive correlation was observed between K_{Ca} conductance and oscillation frequency. **(D)** An almost linear negative correlation was noticed between K_A conductance and oscillation frequency. **(E)** A negative correlation was seen between K_{Dr} conductance and oscillation frequency. **(F)** An inverted-U correlation was observed between leak conductance and oscillation frequency. **(G)** A bimodal correlation with two peaks was noticed between Na conductance and oscillation frequency. **(H)** No correlation was seen between Ca_S conductance and oscillation frequency.

Problems Encountered

The most impactful problem was seen because the E_{leak} of the example neuronal cell (-50mV) differs from the E_{leak} that was chosen for this project (-60mV). This change was made for a couple reasons, one of which being that I, personally, wanted to learn more about the subject and figured that I wouldn't learn much about the process if I simply modified the parameters given to fit within the example bounds that were provided. The example parameter bounds were still helpful and could be followed for the most part, but some deviations and additional research had to be done in order to get a satisfactory result.

Over the course of developing this computational model, one problem in particular continued to appear. The core of this problem was unrealistic parameters. Unrealistic parameters

are incredibly harmful when developing computational models of neurons, especially when you aren't basing your model off of a specific neuron, like was done in this project. Because between each stage of development there are often multiple conductances and other additional parameters being altered, getting stuck in a 'local minimum' of parameters is especially easy to do. This was especially noticeable with the hyperpolarizing current's conductance when completing the final stage of development, introducing the rebounding-burst pattern. This problem was mostly mitigated by simply basing the parameters off of real neuronal cells' parameters which have similar function to our own.

When it comes to fine-tuning parameters, some sets of parameters formed a special relationship. The first of which was those concerned with the dynamics of the calcium pool. Tau_{Ca}, F_{Ca}, and the conductances of K_{Ca} , Ca_S, and Ca_T, fall into this category. Finding a balance between the Ca influx (caused by Ca_S and Ca_T) and the Ca efflux (caused by Tau_{Ca}) was especially difficult, as they not only influence the Ca pool but also have highly impactful effects on the dynamics of the adapting and bursting patterns. In addition to affecting the Ca pool, the Ca_T currents had an were antagonistically effected by K_D currents. The heart of this relationship is because Ca_T is responsible for burst initiation and K_D is responsible for burst suppression. Balance of these two variables heavily determined the systems ability to escape inhibition and initiate bursts. In addition to this, Ca_S and K_A formed a similar opposing relationship, as Ca_S sustains a bursting state and K_A incentivizes limiting of a burst. This interaction shapes burst dynamics by controlling burst duration and intensity.

Appendix

The full computational implementation of the single-cell and two-cell half-center oscillator models was developed using NEURON with Python. Due to the length and modular structure of the codebase, which includes multiple .mod files for ion channel definitions, the complete, fully documented code is provided electronically. The Google Colab notebook contains the testing and analysis code, including simulation execution, parameter sweeps, and graphing routines, while the GitHub repository contains the core model code used to initialize neuronal cells and simulations.

Google Colab (testing, analysis, and visualization):

> https://colab.research.google.com/drive/1WbD1vrt6InEyM2dKCEYecCF8qiXFwOuw?usp=sharing

GitHub repository (model initialization, core code, and back-up version of Colab):

> https://github.com/ibex232/Two-cell-Half-center-Oscillator-Model.git

These resources contain all files required to reproduce the simulations and results presented in this report.